Appl. Phys. B 92, 61–66 (2008)
DOI: 10.1007/s00340-008-3055-x

Applied Physics B
Lasers and Optics

L.A. GÓMEZ[1]
C.B. DE ARAÚJO[1,✉]
A.M. BRITO-SILVA[2]
A. GALEMBECK[3]

Solvent effects on the linear and nonlinear optical response of silver nanoparticles

[1] Departamento de Física, Universidade Federal de Pernambuco, 50670-901 Recife, PE, Brazil
[2] Programa de Pós-Graduação em Ciência de Materiais, Universidade Federal de Pernambuco, 50670-901 Recife, PE, Brazil
[3] Departamento de Química Fundamental, Universidade Federal de Pernambuco, 50670-901 Recife, PE, Brazil

Received: 24 March 2008
Published online: 4 June 2008 •

ABSTRACT Linear and nonlinear (NL) optical properties of silver colloids stabilized with poly(N-vinylpyrrolidone) (PVP) in water, acetone, methanol, and ethylene glycol were studied. Images obtained by transmission electron microscopy reveal narrow size distributions of silver nanoparticles (NPs) with diameters centered at ≈ 6.3 nm (aqueous colloid) and in the 4.3–4.9 nm range for the other colloids. The behavior of the surface plasmon resonance band associated with the NPs was monitored through the linear absorption spectrum, and its dependence on the linear refraction index and the electric dipole moment (EDM) of the solvent molecules was analyzed. The phenomenological parameter, A, obtained from the linear absorption spectra, includes contributions due to the surface effects and the solvent. The third order susceptibility of the colloid was measured using the Z-scan technique at 532 nm, and the NL optical susceptibility of the NPs was determined using the Maxwell–Garnett model. The results indicate that the NL response of the colloids is largely influenced by the molecules adsorbed on the NPs surfaces and the EDM of the solvent molecules.

PACS 42.65.-k; 42.65.An; 73.20.Mf; 78.67.-n; 78.67.Bf; 82.70.Dd

1 Introduction

Metallic nanoparticles (NPs) present a surface plasmon resonance (SPR) wavelength and lineshape that depends upon their size and shape, and the medium they are embedded in [1–6]. This sensitivity with respect to the surrounding medium allows for the development of SPR sensing devices for measurements of physical quantities, and chemical- and bio-sensing [7].

Normally, the NPs environment in colloidal systems is composed of the solvent and stabilizing agents adsorbed on the NPs surface to avoid aggregation. The solvent and the stabilizing agent may change the optical properties of the NPs in different ways. In the case of stabilizing agents, the adsorbed molecules (AM) may cover the NPs as a shell, changing the NPs dielectric function, $\varepsilon_{\mathrm{m}}(\lambda) = \varepsilon'_{\mathrm{m}}(\lambda) + \mathrm{i}\varepsilon''_{\mathrm{m}}(\lambda)$, where λ is the light wavelength. However, changes in the dielectric function of the solvent, $\varepsilon_{\mathrm{h}}(\lambda)$, modify the SPR condition that corresponds to $\varepsilon'_{\mathrm{m}}(\lambda_{\mathrm{SP}}) + 2\,\mathrm{Re}\,\varepsilon_{\mathrm{h}}(\lambda_{\mathrm{SP}}) = 0$, where λ_{SP} is the SPR wavelength [1, 2].

Many authors studied metallic colloids prepared chemically or by laser ablation in different solvents [8–14], by analyzing the effect of particle geometry and the contributions of the AM to the linear optical properties [15, 16]. The dependence of the nonlinear (NL) properties was studied as a function of the NPs shape [17–19] and size [20, 21]. Recently, the influence of AM on the third-order susceptibility of the NPs, $\chi^{(3)}_{\mathrm{m}}$, was studied for the first time [22]. The NPs were capped with sodium citrate, poly(N-vinylpyrrolidone) (PVP) and polyvinyl alcohol (PVA), and the NL experiments revealed that $|\chi^{(3)}_{\mathrm{m}}|$ changes by more than 100% for the different stabilizing agents. However, the influence of the host has not been studied in detail. In particular the contribution of the electric dipole moment (EDM) of the solvent molecules was not considered in the majority of the papers. In fact the EDM may change the electron density on the NPs surface, and therefore their dielectric response can be largely modified [14].

In this work we investigated the influence of the linear refractive index and the EDM of the solvent on the optical properties of colloidal silver. Samples containing silver NPs stabilized with PVP in different media (water, acetone, methanol and ethylene glycol) were prepared and characterized by linear absorption spectroscopy, transmission electron microscopy and by an NL optical technique. The effective third-order susceptibility, $\chi^{(3)}_{\mathrm{eff}}$, was measured for all colloids and the results were used to determine the NL susceptibility of the NPs. The calculations of $\chi^{(3)}_{\mathrm{m}}$ were made using the generalized Maxwell–Garnet model [23] and the results are discussed considering the solvent influence on the NL response. The present results show that besides the influence of the stabilizing agents on the susceptibility of the NPs, as previously reported in [22], the refractive index and the EDM of the solvent molecules also affect very much of the value of $\chi^{(3)}_{\mathrm{m}}$.

2 Experimental details

Colloids stabilized with PVP were prepared as follows: a 1.4 ml portion of $AgNO_3$ in methanol (4.71×10^{-2} mol l^{-1}) was mixed with 0.25 g of PVP and 0.011 g of

✉ E-mail: cid@df.ufpe.br

sodium borohydride ($NaBH_4$) in 250 ml of each solvent (water, acetone, methanol and ethylene glycol). In all cases the final solution was stirred and boiled for 1 h to decompose any excess $NaBH_4$. Colloids obtained by this method have a broad NPs size distribution.

Subsequently, 1 ml of each colloid prepared was ablated using the second harmonic from a Q-switched Nd:YAG laser (532 nm, 10 Hz, 8 ns) for 30 min. Laser ablation of NPs in colloids prepared by chemical synthesis has been studied by different authors and the procedure of [25–27] was properly adapted in the present case to achieve nearly the same average particle size with narrow distribution for the samples synthesized in different liquids. The shape and size of the silver NPs in the laser-ablated colloids were determined using a transmission electron microscope operating at 80 kV. NPs with a narrow size distribution were observed in all samples at the end of the ablation process.

Absorption spectra from 200 to 700 nm were recorded using a diode array spectrophotometer with the colloid contained inside a 5 mm thick quartz cell. The spectra did not change during the observation period of about one month indicating that the colloids have large stability.

The NL experiments were performed with the second harmonic beam (at 532 nm) obtained using a Q-switched and mode-locked Nd:YAG laser and a KTP crystal. Single pulses of 80 ps at 6 Hz and peak intensity of 0.9 GW/cm^2 were selected using a pulse picker system. The signals were recorded using a boxcar connected to a computer.

3 Results and discussion

Figure 1 shows a representative micrograph of the laser-ablated colloid and the corresponding NPs size distribution. The solid line is a log-normal distribution which gives the average diameter of $\approx 4.9 \pm 1.2$ nm for NPs in methanol. Similar result was obtained for acetone while the average diameter was 4.3 ± 2.5 nm in ethylene glycol and 6.3 ± 2.7 nm for NPs in water.

The absorbance spectra of the silver colloids are shown in Fig. 2. In general, the changes in the SPR wavelength and lineshape can be ascribed to size and shape of the NPs, and the host characteristics. A red shift of λ_{SP} is observed when the linear refractive index of the host is increased. The shape of the NPs changes the resonance condition to $\varepsilon'_m(\lambda_{SP}) + \xi \operatorname{Re} \varepsilon_h(\lambda_{SP}) = 0$, where ξ depends on the geometry of the NPs. For example, $\xi = 2$ for spherical NPs, and $\xi \approx 16$ for ellipsoidal NPs with an aspect ratio of 5 : 1 [28]. In the present case the NPs are considered spherical. The changes of the NPs dielectric constant due to the NPs size can be modeled as $\varepsilon_m(\lambda) = \varepsilon'_{m,bulk}(\lambda) + i\{\varepsilon''_{m,bulk}(\lambda) + (\omega_p^2/\omega^3)(A v_F/R)\}$, where v_F is the Fermi velocity, ω_p is the plasma frequency, R is the particle radius, and A is a phenomenological parameter that has physical origin in the scattering of electrons with the NPs walls [29]. The molecules chemically bounded to the NPs' surface change their dielectric constant; this effect may be considered using a core-shell model [19]. However, as the thickness of the shell and its dielectric constant are unknown, the corrections in the dielectric constant of the NPs are considered using the A-parameter. When surface effects are not taken into account $A = 1$ but the presence of adsorbed molecules on the NPs surface may change A by a large amount. For example A can be a complex number where the imaginary (Im A) and real (Re A) parts are associated with the shift and the broadening in the SPR, respectively.

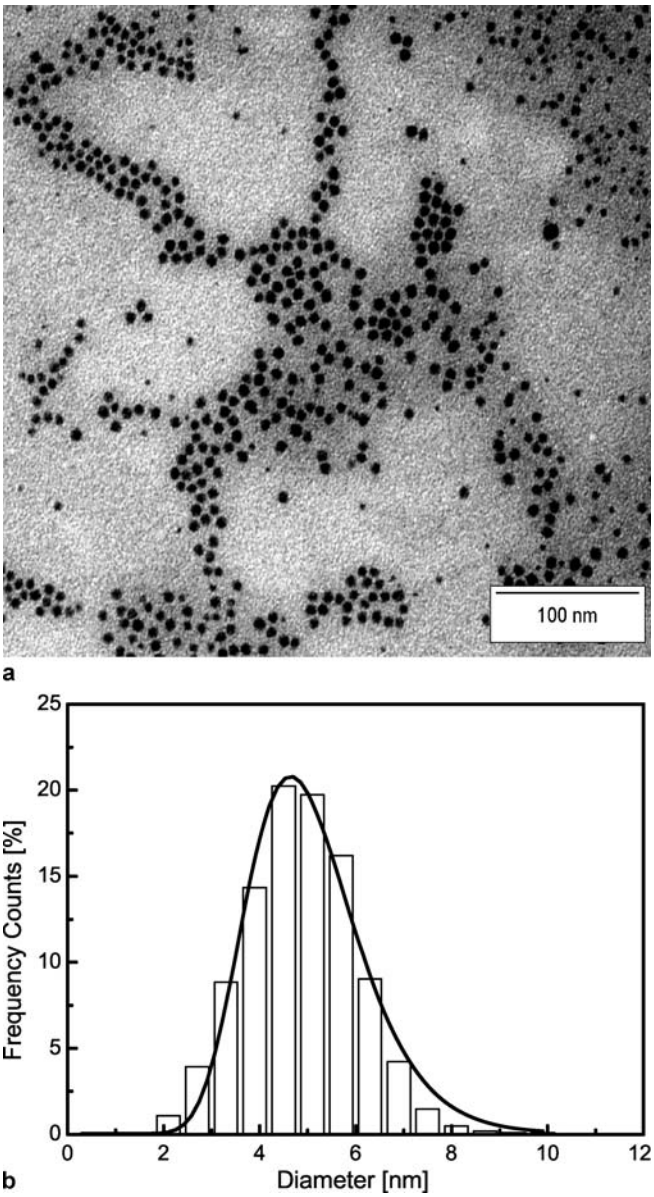

FIGURE 1 TEM images (**a**) and NPs size distribution (**b**) of silver NPs in methanol. The average size of 4.9 ± 1.2 nm was obtained by adjusting a log-normal curve to the histogram

In order to characterize the contribution of the environment and NPs size, a theoretical SPR lineshape was calculated using the Mie theory [1, 2]. The extinction coefficient of the colloid can be written as

$$\alpha = \frac{18\pi f}{\lambda} \varepsilon_h(\lambda)^{3/2} \frac{\varepsilon''_m(\lambda)}{(\varepsilon'_m(\lambda) + 2\varepsilon_h(\lambda))^2 + \varepsilon''^2_m(\lambda)}, \quad (1)$$

where f is the filling fraction (the fraction of the total volume occupied by the NPs). But, in order to compare α with the experimental results, the phenomenological parameter A is introduced in the expression of $\varepsilon_m(\lambda)$ as indicated above. Fitting equation (1) for α and $\varepsilon_m(\lambda)$, using the bulk silver

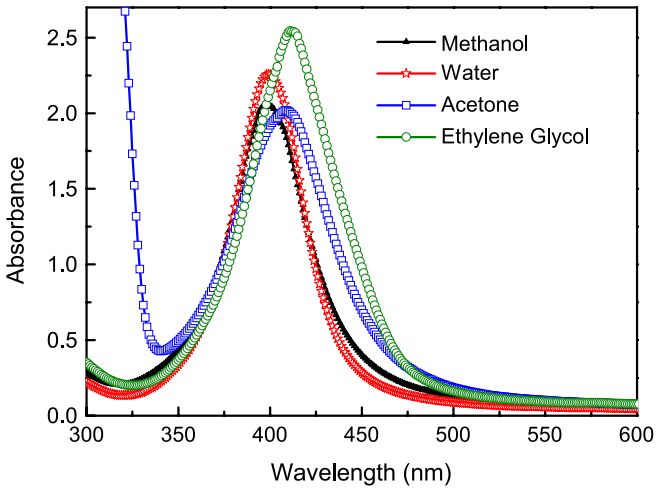

FIGURE 2 Absorbance spectra of the laser ablated silver colloids stabilized with PVP. Sample thickness: 5 mm

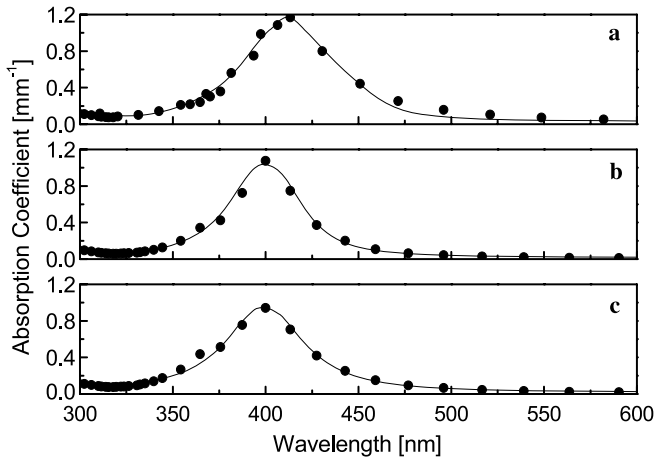

FIGURE 3 Absorption coefficient and lineshape of the surface plasmon resonance for silver NPs in (**a**) ethylene glycol, (**b**) water and (**c**) methanol. The *points* are the fitting results using (1). It was observed that changes of A by 10% does not affect the agreement with the experiment

parameters [30], we determined A and f for each sample. Different values of A were obtained, indicating that surface effects contribute in different ways in each colloid. The analysis was performed for all samples that have linear refractive index, EDM, SPR wavelength, f and A as given in Table 1. The value of f was confirmed with the stoichiometric analysis of the solution assuming that all silver ions were reduced.

Figure 3 shows the best fit of the SPR lineshape for silver NPs in ethylene glycol, water and methanol. The fitting parameters are the real and the imaginary parts of A that varies

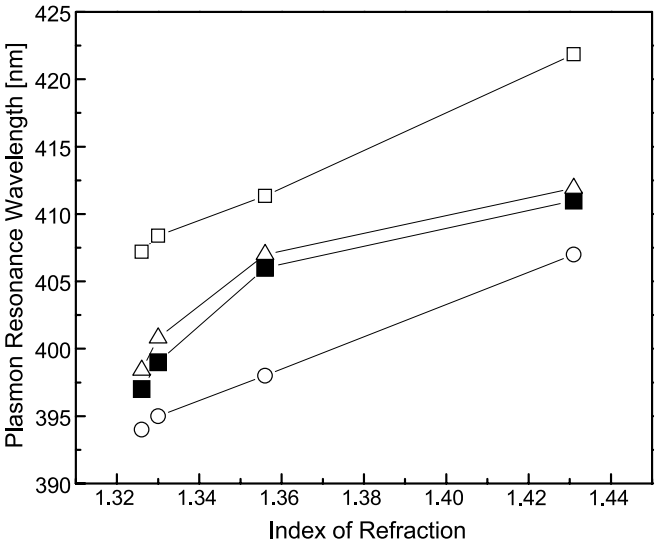

FIGURE 4 Surface plasmon resonance wavelength as a function of the linear refraction index. *Open circles* were calculated using bulk values for the dielectric function of silver, neglecting surface effects. *Open squares* correspond to $A = 1$ and *open triangles* were obtained using the corresponding values of A indicated in Table 1. The *solid squares* refer to the experimental results

as $0.19 < \mathrm{Re}\, A < 0.45$ and $0.31 < \mathrm{Im}\, A < 0.58$. Good results for the SPR lineshape were also obtained for the other samples. An analysis of the influence of the scattering parameter A is presented in Fig. 4 where deviations from the experimental λ_{SP} under different assumptions are observed. The open circles correspond to the λ_{SP} values calculated using the bulk dielectric function of silver, $\varepsilon_{m,bulk}$ [30]. The influence of the NPs size on λ_{SP} is illustrated by the open squares obtained assuming $A = 1$, neglecting the solvent effects and in this case $\varepsilon''_m > \varepsilon''_{m,bulk} \approx 0$. Surface effects were considered using the A values given in Table 1, obtained from the best fit illustrated in Fig. 3. The surface plasmon resonance condition, $\varepsilon'_m(\lambda_{SP}) + 2\,\mathrm{Re}\,\varepsilon_h(\lambda_{SP}) = 0$, is determined using $\varepsilon'_m(\lambda) = \varepsilon'_{m,bulk}(\lambda) - (\mathrm{Im}\, A)(\omega_p^2/\omega^3)(\nu_F/R)$. Deviations from the theoretical results corresponding to $\varepsilon_{m,bulk}$ from the SPR wavelength are larger for solvents with high EDM. This is observed for acetone and ethylene glycol that correspond to $|A|$ larger than for the others solvents. These results indicate that solvents with high EDM interact strongly with the electron distribution on the NPs surface. Notice that ethylene glycol has a larger index of refraction than acetone but the value of $|A|$ for acetone is larger by $\sim 25\%$.

The third order susceptibilities of the colloids were determined using the Z-scan technique [31]. For the NL measurements the sample is mounted in a translation stage which

Host	Index of refraction	Electric dipole moment [D]	SPR wavelength, λ_{SP} [nm]	f [$\times 10^{-6}$]	A	$\lvert A\rvert$
Methanol	1.326	1.70*	397	3.1	$0.40 - i0.35$	0.53
Water	1.333	1.85*	399	2.7	$0.19 - i0.45$	0.49
Acetone	1.356	2.88**	407	3.2	$0.40 - i0.55$	0.68
Ethylene glycol	1.431	2.28*	411	3.4	$0.45 - i0.31$	0.55

* see [38]
** see [39]

TABLE 1 Linear index of refraction, electric dipole moment of the molecules, experimental surface plasmon resonance (SPR) wavelength, λ_{SP}, NPs filling fraction, f, and scattering parameter, A, used to fit the SPR lineshape

moves along the beam propagation direction (Z axis). The laser beam is focused with a 10 cm focal length lens. Prefocal and postfocal positions correspond to negative and positive values of Z, respectively. The light beam crossing the sample pass through an aperture of radius r_a placed in the far-field region, being detected by a photodiode connected to a boxcar and a computer. To detect variations in the light wavefront due to the NL refractive index, n_2, the aperture radius must be smaller than the beam waist w_a in the aperture position (closed-aperture scheme). The ratio between the intensity transmitted through the aperture and the incident intensity in the aperture is given by $S = \{1 - \exp(-2r_a^2/w_a^2)\}$. For the present work $S = 0.02$ was used. When the transmitted light is unblocked ($S = 1$) the NL absorption coefficient, α_2, is determined (open-aperture scheme). To compensate for fluctuations in the laser intensity, a reference channel was used to improve the signal-noise ratio as originally introduced in [32]. Changes in the normalized transmittance, ΔT, are proportional to the NL coefficients. For $S < 1$ we have $\Delta T = 0.406 k L_{\text{eff}} n_2 I$ and for $S = 1$, $\Delta T = \alpha_2 I L_{\text{eff}}/2^{1.5}$, where $k = 2\pi/\lambda$, $L_{\text{eff}} = [1 - \exp(-\alpha L)]/\alpha$, L is the sample length and I is the laser intensity.

The experiments were performed with colloids having f varying from 2.7×10^{-6} to 3.4×10^{-6}. Figure 5 shows the Z-scan traces for silver NPs in ethylene glycol, water and methanol. The experiments were performed with a laser wavelength off-resonance with the surface plasmon band. Moreover, the laser repetition rate was very small (6 Hz) to prevent the influence of thermal effects. The Z-scan measurements were made in a single run. For each sample translation of 0.3 mm the transmitted intensity averaging over 20 laser shots using a boxcar integrator was measured. This corresponds to 2000 measurements of intensity in a single run. Then, from the Z-scan profiles, n_2 and α_2 were calculated using the procedure of [31] and the results were used to determine

$$\text{Re}\left[\chi_{\text{eff}}^{(3)}\right] = \frac{4\varepsilon_0 n_0^2 c}{3} n_2 [\text{m}^2/\text{W}]$$

and

$$\text{Im}\left[\chi_{\text{eff}}^{(3)}\right] = \frac{2\varepsilon_0 n_0^2 c^2}{3\omega} \alpha_2 \,[\text{m/W}],$$

where n_0 is the linear refraction index, ω is the laser frequency, c is the speed of light in vacuum and ε_0 is the vacuum permittivity. Negative values of n_2 (defocusing nonlinearity) and positive values of α_2 (two-photon absorption) were obtained. These parameters allow for the calculation of the NPs susceptibilities by considering an appropriate model to describe

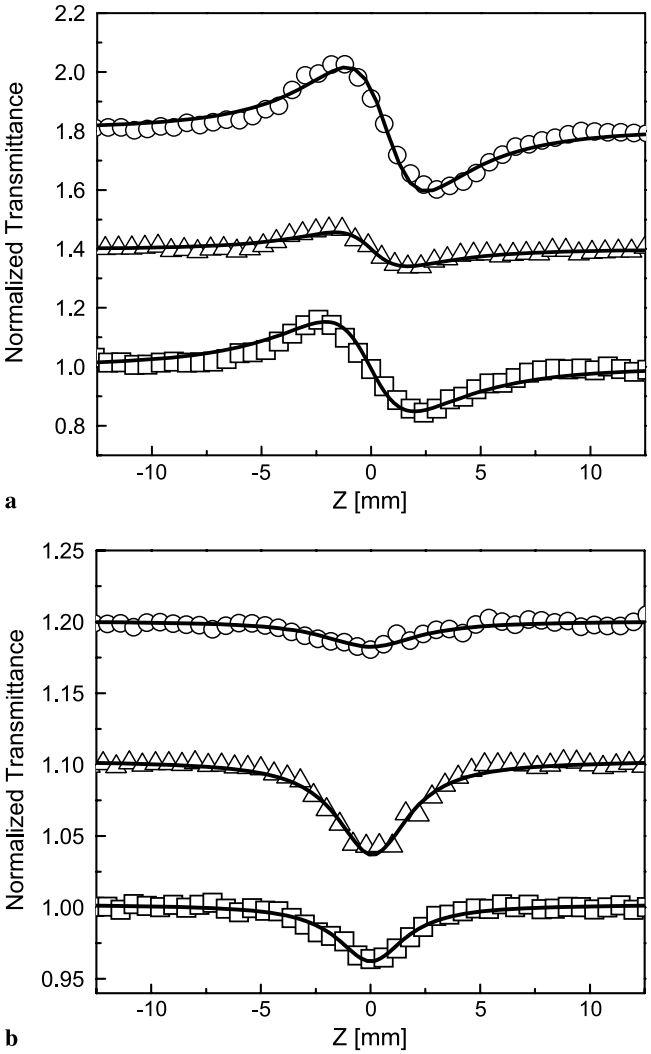

FIGURE 5 Z-scan traces for silver NPs in acetone (*open circles*), water (*open triangles*) and methanol (*open squares*). (**a**) $S = 0.02$ and (**b**) $S = 1$. A shift was introduced in the curves baselines to prevent overlap among them

the colloid. It is well known that, depending on the sample constituents, $\chi_{\text{eff}}^{(3)}$ is affected in different ways. The results obtained for n_2, α_2 and $\chi_{\text{eff}}^{(3)}$ are given in Table 2. Note that $\text{Im}\,\chi_{\text{eff}}^{(3)} \ll \text{Re}\,\chi_{\text{eff}}^{(3)}$ for all colloids studied.

The generalized Maxwell–Garnett (MG) model [23] was applied to determine the value of $\chi_{\text{m}}^{(3)}$ in the presence of each solvent. The MG model has been successfully used for metallic colloids [21, 33–35] and is appropriate

Host	n_2 [10^{-14} cm^2/W]	α_2 [10^{-10} cm/W]	Local field factor, $\lvert\eta\rvert$	Re[$\chi_{\text{eff}}^{(3)}$] [10^{-20} m^2/V^2]	Im[$\chi_{\text{eff}}^{(3)}$] [10^{-22} m^2/V^2]	Re[$\chi_{\text{m}}^{(3)}$] [10^{-15} m^2/V^2]	Im[$\chi_{\text{m}}^{(3)}$] [10^{-15} m^2/V^2]	$\lvert\chi_{\text{m}}^{(3)}\rvert$ [10^{-15} m^2/V^2]
Methanol	−1.61	2.02	0.862	−1.00	5.32	−4.89	3.63	6.09
Water	−0.57	3.99	0.893	−0.36	10.6	−1.80	1.43	2.30
Acetone	−2.47	1.10	0.989	−1.62	3.05	−4.58	3.55	5.80
Ethylene glycol	−5.18	2.28	1.108	−3.76	6.99	−5.77	4.56	7.36

TABLE 2 Nonlinear parameters: $\chi_{\text{eff}}^{(3)}$ is the effective susceptibility; n_2 is the NL refractive index; α_2 is the NL absorption coefficient; $\chi_{\text{m}}^{(3)}$ is the NL susceptibility of silver nanoparticles in different media, and η is the local field factor. The estimated error in the $\lvert\chi_{\text{m}}^{(3)}\rvert$ values is ±15%

to describe the present system. For composites, with diluted spherical inclusions dispersed in a uniform solvent with $f \ll 1$, we have: $\chi^{(3)}_{\text{eff}} = f\eta^2|\eta|^2\chi^{(3)}_{\text{m}} + \chi^{(3)}_{\text{h}}$, where $\eta = 3\varepsilon_{\text{h}}(\lambda)/[\varepsilon_{\text{m}}(\lambda) + 2\varepsilon_{\text{h}}(\lambda)]$ is the local field factor inside the NPs and $\chi^{(3)}_{\text{h}}$ is the NL susceptibility of the solvent. The model allows, for example, to describe how the NL response can be affected by interferences between the real and the imaginary parts of the NL susceptibilities associated to the colloid constituents, showing cancellation and sign reversal of n_2 [35] and α_2 [34].

The values of $|\eta|$ for all samples are indicated in Table 2 together with the parameters obtained from the present NL measurements. The solvents used are transparent and have negligible nonlinearity ($2.5 \times 10^{-22}\,\text{m}^2/\text{V}^2 < \chi^{(3)}_{\text{h}} < 1.5 \times 10^{-21}\,\text{m}^2/\text{V}^2$) [36, 37]. Therefore the important contribution for $\chi^{(3)}_{\text{eff}}$ originates from the NL polarization induced in the NPs.

From Table 2 one can see that the NL parameters for the silver NPs in the aqueous colloid are in agreement with previous results [21, 24], taking into account the average diameter of the NPs in the experiments. However, disagreements with predictions based on the models available in the literature are observed. For example, according to [1], the SPR position of identical NPs in colloids with the same $\varepsilon_{\text{h}}(\lambda)$ must be the same and similar NL results would be expected for colloids with approximate index of refraction such as acetone, water and methanol. However, as can be seen, this is not the case. Table 2 shows large variation of the $|\chi^{(3)}_{\text{m}}|$ values from $2.30 \times 10^{-15}\,\text{m}^2/\text{V}^2$ to $6.09 \times 10^{-15}\,\text{m}^2/\text{V}^2$. The influence of the EDM has to be the reason for such large range of values. However, a comparison between the results for ethylene glycol and acetone shows an increase of $|\chi^{(3)}_{\text{m}}|$ although the EDM of ethylene glycol is smaller than for acetone. The influence of the EDM very much affects the electron density of states of the NPs. These results indicate that it is important to take into account the different values of the EDM of the molecules in the solvent. It is also important to recall that the local field factor, η, is dependent on A through the NPs dielectric function. Note that the values of $|\eta|$ for all solvents increases with the increase of the refraction indices. We also observe that the values of $|\chi^{(3)}_{\text{m}}|$ are correlated with Re A. The correlation between the local field factor η and the EDM of the molecules with $\chi^{(3)}_{\text{m}}$ determines the nonlinearity of the composite in such way that values of $|\chi^{(3)}_{\text{m}}|$ differing by up to $\sim 300\%$ were obtained. However, the details of the contribution due to electrons in the NPs, the role of the dipolar layer due to AM and the EDM of the solvent molecules cannot be completely understood at the present time. The herein reported results indicate clearly the need for corrections in published models describing the nonlinearity of silver colloids that only take into account the contribution of NPs carriers for the NL susceptibility.

4 Summary

The linear and NL optical properties of silver colloids prepared with different solvents were investigated. Changes in the wavelength and lineshape of the SPR due to the solvent were analyzed to determine the scattering parameter, A. It was observed that solvents with molecules presenting large electric dipole moment significantly change the linear and NL response of the metallic colloid. In the linear case the value of $|A|$ changed by more than 35% for the various solvents studied. Large variations of the silver NPs susceptibility of $\sim 300\%$ were determined based on the generalized Maxwell–Garnet model.

ACKNOWLEDGEMENTS Financial support by the Brazilian agencies Conselho Nacional de Desenvolvimento Científico e Tecnológico (CNPq), Coordenação de Aperfeiçoamento de Pessoal de Nível Superior (CAPES) and Fundação de Amparo a Ciência e Tecnologia do Estado de Pernambuco (FACEPE) is acknowledged. This work was performed under the Millenium Institute (Nonlinear Optics, Photonics and Bio-Photonics) Project and the Nanophotonics Network Program.

REFERENCES

1 See for example: S. Link, M.A. El-Sayed, Annu. Rev. Phys. Chem. **54**, 331 (2003)
2 S. Link, M.A. El-Sayed, J. Phys. Chem. B **103**, 4212 (1999) and references therein
3 J.J. Mock, M. Barbic, D.R. Smith, D.A. Schultz, S. Schultz, J. Chem. Phys. **116**, 6755 (2002)
4 H. Hövel, S. Fritz, A. Hilger, U. Kreibig, M. Vollmer, Phys. Rev. B **48**, 18 178 (1993)
5 J.J. Mock, D.R. Smith, S. Schultz, Nano Lett. **3**, 485 (2003)
6 T.R. Jensen, M.L. Duval, K.L. Kelly, A.A. Lazarides, G.C. Schatz, R.P. Van Duyne, J. Phys. Chem. B **103**, 9846 (1999)
7 A. Curry, G. Nusz, A. Chilcoti, A. Wax, Appl. Opt. **46**, 1931 (2007) and references therein
8 R.A. Ganeev, M. Baba, A.I. Ryasnyansky, M. Suzuki, H. Kuroda, Opt. Commun. **240**, 437 (2004)
9 R. Brause, H. Möltgen, K. Kleinermanns, Appl. Phys. B **75**, 711 (2002)
10 V.A. Karavanskii, A.V. Simakin, V.I. Krasovskii, P.V. Ivanchenko, Quantum Electron. **34**, 644 (2004)
11 M.H.G. Miranda, E.L. Falcão-Filho, J.J. Rodrigues Jr., C.B. de Araújo, L.H. Acioli, Phys. Rev. B **70**, 161 401(R) (2004)
12 R.A. Ganeev, A.I. Ryasnyansky, S.R. Kamalov, M.K. Kodirov, T. Usmanov, J. Phys. D **34**, 1602 (2001)
13 Y.P. Sun, J.E. Riggs, H.W. Rollins, R. Guduru, J. Phys. Chem. B **103**, 77 (1999)
14 R.M. Tilaki, A. Irajizad, S.M. Mahdavi, Appl. Phys. A **84**, 215 (2006)
15 J. Kottmann, O. Martin, D. Smith, S. Schultz, Opt. Express **6**, 213 (2000)
16 P. Mulvaney, Langmuir **12**, 788 (1996)
17 N. Okada, Y. Hamanaka, A. Nakamura, I. Pastoriza-Santos, L.M. Liz-Marzan, J. Phys. Chem. B **108**, 8751 (2004)
18 J. Jayabalan, A. Singh, R. Chari, S.M. Oak, Nanotechnology **18**, 315 704 (2007)
19 A. Neeves, M.H. Birnboim, J. Opt. Soc. Am. B **6**, 787 (1989)
20 K. Uchida, S. Kaneko, S. Omi, C. Hata, H. Tanji, Y. Asahara, A.J. Ikushima, T. Tokizaki, A. Nakamura, J. Opt. Soc. Am. B **11**, 1236 (1994)
21 V.P. Drachev, A.K. Buin, H. Nakotte, V.M. Shalaev, Nano Lett. **4**, 1535 (2004)
22 L.A. Gómez, A.M. Brito-Silva, C.B. de Araújo, A. Galembeck, J. Opt. Soc. Am. B **24**, 2136 (2007)
23 J.W. Sipe, R.W. Boyd, Phys. Rev. A **46**, 1614 (1992)
24 Y. Deng, Y. Sun, P. Wang, D. Zhang, X. Jiao, H. Ming, Q. Zhang, Y. Jiao, X. Sun, Curr. Appl. Phys. **8**, 13 (2008)
25 P.V. Kamat, M. Flumiani, G.V. Hartland, J. Phys. Chem. B **102**, 3123 (1998)
26 A. Takami, H. Kurita, S. Koda, J. Phys. Chem. B **103**, 1226 (1999)
27 S. Link, C. Burda, M.B. Mohamed, B. Nikoobackht, M.A. El-Sayed, J. Phys. Chem. A **103**, 1165 (1999)
28 A.D. McFarland, R.P. Van Duyne, Nano Lett. **3**, 1057 (2003)
29 A. Pinchuck, U. Kreibig, A. Hilger, Surf. Sci. **557**, 269 (2004)
30 E.D. Palik, *Handbook of Optical Constants of Solids* (Academic, New York, 1985)
31 M. Sheik-Bahae, A.A. Said, T. Wei, D.J. Hagan, E.W. Van Stryland, IEEE J. Quantum Electron. **QE-26**, 760 (1990)

32 H. Ma, A.S. Gomes, C.B. de Araújo, Appl. Phys. Lett. **59**, 2666 (1991)
33 D. Ricard, P. Roussignol, C. Flytzanis, Opt. Lett. **10**, 511 (1985)
34 D.D. Smith, G. Fischer, R.W. Boyd, D.A. Gregory, J. Opt. Soc. Am. B **14**, 1625 (1997)
35 E.L. Falcão-Filho, C.B. de Araújo, A. Galembeck, M.M. Oliveira, A.J.G. Zarbin, J. Opt. Soc. Am. B **22**, 2444 (2005)
36 R.L. Sutherland, *Handbook of Nonlinear Optics* (Marcel Decker, New York, 1996)
37 K.L. Schehrer, E.S. Fry, J. Opt. Soc. Am. B **6**, 1182 (1989)
38 K.A. Fletcher, I.A. Storey, A.E. Hendricks, S. Pandey, S. Pandey, Green Chem. **3**, 210 (2001)
39 N.I. Hammer, R.N. Compton, L. Adamowicz, S.G. Stepanian, Phys. Rev. Lett. **94**, 153 004 (2005)